Black Phosphorus

International Edition: DOI: 10.1002/anie.201605168
German Edition: DOI: 10.1002/ange.201605168

Light-Induced Ambient Degradation of Few-Layer Black Phosphorus: Mechanism and Protection

Qionghua Zhou, Qian Chen, Yilong Tong, and Jinlan Wang**

Abstract: *The environmental instability of single- or few-layer black phosphorus (BP) has become a major hurdle for BP-based devices. The degradation mechanism remains unclear and finding ways to protect BP from degradation is still highly challenging. Based on ab initio electronic structure calculations and molecular dynamics simulations, a three-step picture on the ambient degradation of BP is provided: generation of superoxide under light, dissociation of the superoxide, and eventual breakdown under the action of water. The well-matched band gap and band-edge positions for the redox potential accelerates the degradation of thinner BP. Furthermore, it was found that the formation of P-O-P bonds can greatly stabilize the BP framework. A possible protection strategy using a fully oxidized BP layer as the native capping is thus proposed. Such a fully oxidization layer can resist corrosion from water and leave the BP underneath intact with simultaneous high hole mobility.*

Single- or few-layer black phosphorus (BP, termed as phosphorene),[1] as one of the most promising two-dimensional (2D) semiconductors for electronic and optoelectronic device applications, has attracted tremendous interest recently. The most distinguished virtues of phosphorene lie in its tunable direct band gap, high carrier mobility, and moderate on/off ratio, which are hard to achieve simultaneously by either graphene or monolayer transition metal dichalcogenides.[1a,2] However, fast oxidation and light-induced degradation of exfoliated flakes of BP in air moisture conditions have been widely reported and the degradation mechanism has been highly debated.[3] Castellanos-Gomez et al. attributed the degradation to the intrinsically hydrophilic of BP surface,[3a] while Ziletti et al. believed that oxygen is the main reason, the triplet-to-singlet conversion greatly lowers the oxygen dissociation barrier and the dangling O atoms increases the hydrophilicity of BP surface.[4] Very recently, Favron et al. demonstrated that the degradation is a photoassisted oxidation reaction with oxygen dissolved in the water; oxygen, visible light and water are simultaneously required for the degradation of BP.[5] Nevertheless, Wang et al. held that the degradation of BP is initiated by contact with oxygen, and water does not play a primary role in the reaction.[6] Obviously, the degradation mechanism of BP in ambient conditions is still far from clear.

On the other hand, various capping layers have been implemented to protect the BP against moist air, such as graphene, hexagonal boron nitride (*h*-BN), aluminum oxide (Al_2O_3) layers, surface coordination and covalent functionalization.[7] However, there are still many challenges in preventing the BP flakes from the contamination and damage during the deposition of exotic layers. A very recent study shows that for air exposure a phosphorene oxide forms only at the topmost layer of bulk BP, leaving the deeper layers intact.[8] This offers a great opportunity to use a native oxide layer as a protective layer. Nevertheless, a partial oxidized P_xO_y layer obtained by the oxygen plasma etching serves as a protective layer for three days and eventually starts to degrade.[9] Developing robust native protective routes is thus highly demanding.

In this work, by employing ab initio electronic structure calculations and molecular dynamics simulations, we provide a comprehensive understanding on the ambient degradation of few-layer BP at an atomic level. Our study shows that the degradation involves three important steps (Figure 1 a). The

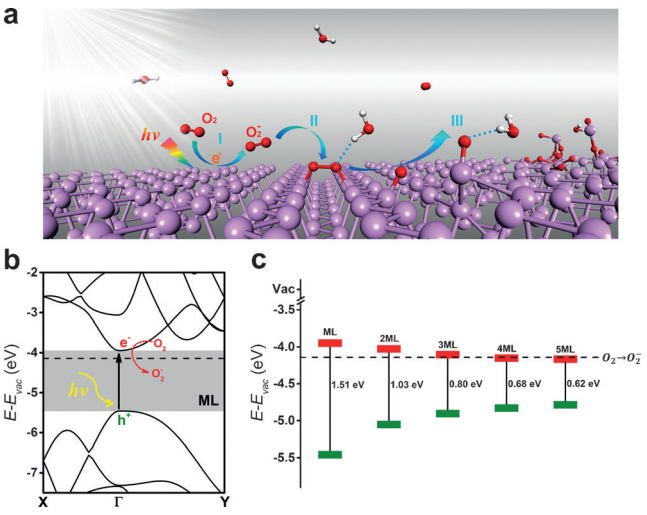

Figure 1. a) The light-induced ambient degradation process of phosphorene. Step I: O_2^- is generated through a charge transfer reaction under ambient light ($O_2 + h\nu \xrightarrow{P} O_2^- + h^+$; P and h^+ stands for phosphorene and a hole, respectively); step II: O_2^- dissociates at the surface and forms two P–O bonds with the phosphorene ($O_2^- + P + h^+ \rightarrow P_xO_y$); step III: through the hydrogen-bond interaction, water molecules draw the bonded O and remove P from the surface and break the top layer of phosphorene. b) HSE band structure for monolayer BP. c) The VBM and CBM of few-layer BP with respect to vacuum energy. The dashed line identifies the redox potential of O_2/O_2^-.

[*] Dr. Q. Zhou, Dr. Q. Chen, Y. Tong, Prof. J. Wang
Department of Physics, Southeast University
Nanjing 211189 (P.R. China)
E-mail: qc119@seu.edu.cn
jlwang@seu.edu.cn

Supporting information for this article can be found under: http://dx.doi.org/10.1002/anie.201605168.

layer-dependent band gaps and conduction band edges are responsible for thickness-dependent degradation observed in few-layer BP. Most importantly, we find that the formation of P-O-P bond can significantly stabilize the BP structure. A possible strategy through fully oxidizing the topmost BP layer as the native capping is therefore proposed. Such a fully oxidized layer can effectively seclude BP from water and thereby prevent further degradation, simultaneously, it leaves the underneath BP intact and maintains comparative hole carrier mobility of BP structure.

All of the ab initio calculations were performed within the framework of density functional theory (DFT) implemented in the Vienna ab initio simulation package (VASP).[10] The Perdew–Burke–Ernzerhof (PBE)[11] and Heyd–Scuseria–Ernzerhof (HSE)[12] exchange-correlation functionals were employed. Van der Waals interactions were considered by the vdW-DF level with the optB88 exchange functional (optB88-vdW)[13] for the geometry optimization. The climbing-image nudged elastic band (CI-NEB) method[14] incorporated with spin-polarized DFT was used to locate the minimum-energy path. Ab initio molecular dynamics (ABMD) simulations were performed at 300 K with a time step of 1.0 fs. More computational details can be found in the Supporting Information.

First, we studied the role of light illumination. It was reported that light illumination is the trigger of the degradation process of phosphorene in ambient conditions.[5] Usually, such light-induced reaction is highly dependent on the band structure of the reactants, such as the water splitting reaction under light. The HSE band structure in Figure 1 b shows that, the valence band maximum (VBM) and conduction band minimum (CBM) of monolayer (ML) BP with respect to vacuum energy are −5.46 and −3.95 eV separately, which gives a direct band gap of 1.51 eV at Γ point. With this sized band gap, the ML BP can produce excitons under ambient light. Furthermore, the redox potential of O_2/O_2^- is just located in the band gap. Thus, the photo-generated electrons can transfer from the conduction band of phosphorene to the O_2 on the surface and generate O_2^-, which are apt to further react with the p-doped phosphorene.

We further calculate the band structures of BP from bilayer (2ML) up to five-layer (5ML), and the valence and conduction band edges with respect to vacuum energy. As shown in Figure 1 c, the band gap decreases gradually as the increase of the layers (from 1.51 eV of ML to 0.62 eV of 5ML) and eventually approaches to the bulk value of 0.37 eV (Supporting Information, Figure S2). The direct influence of this is the difficulty for thicker BP to produce excitons since its band gap is beyond the visible light range. Moreover, the CBM of BP becomes closer and closer to the redox potential of O_2/O_2^- and finally drops below it, which makes the thicker BP hard to produce O_2^-. In particular for bulk BP, it cannot produce O_2^- under ambient conditions at all as its CBM is too low, and it is expected to be rather stable, consistent with the experimental observation.[15] Therefore, the band-gap-dependent exciton generation process combined with the CBM-dependent charge-transfer process makes the thinner BP produce more O_2^- than the thicker BP and eventually accelerates the degradation of thinner BP observed in experiments.[3a,b,5]

We then took a close look at the dissociation process of O_2^-. We chose the situation of one pair of O_2/O_2^- adsorbed onto bilayer BP as an example. For the sake of clarity, we let the O_2/O_2^- lie above the zigzag valley and parallel to the surface, which is one of the energetically favorable configurations.[4] The O_2^- is physisorbed on BP surface with a distance of 2.4 Å (for details, see the Supporting Information, Figure S4 and Table S2). The adsorption energy is 0.92 eV which is about four times larger than that of the neutral O_2 (0.19 eV). Therefore, for thinner BP which produces more O_2^-, the adsorption of O_2^- is robust and hard to desorb, which is beneficial to higher oxygen concentration on the surface. On the contrary, the thicker BP produces few O_2^- and the adsorbate is mainly O_2 which are weakly adsorbed and easy to desorb. This is in accordance with the experimental observation that thinner region contains higher oxygen concentration.[5]

To form phosphorene oxide, dissociation of O_2 or O_2^- is required. It is well-known that the unpaired triplet state is the ground state of gaseous oxygen. In our calculations, the physisorbed O_2/O_2^- is still in its molecular ground state. With more and more close to the phosphorene surface, the O–O bond length is enlarged and a P–O chemical bonding is formed (Figure 2 a; Supporting Information, Table S2). Correspondingly, the chemisorbed O no longer keeps its spin-parallel ground state. This triplet-to-singlet conversion proposed by previous study[4] lowers the reaction barrier to 0.56 eV for O_2 adsorbed onto the bilayer BP. A similar process happens for O_2^-, and the barrier even lowers to 0.4 eV. It should be noted that the bilayer BP is hole doped by the light excitation, which was not included in our calculation. In other

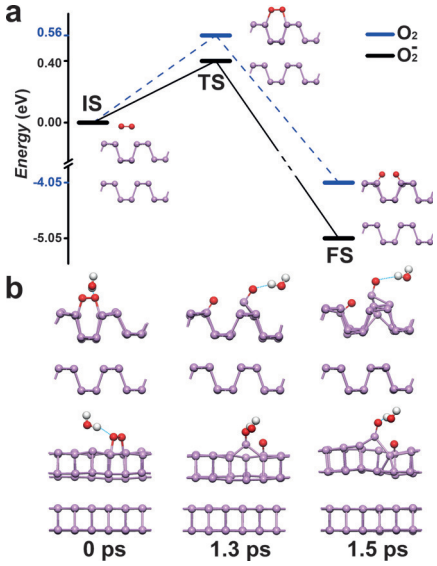

Figure 2. The oxidization and disintegration process of bilayer BP. a) Reaction path for O_2^- (black) and O_2 (blue) adsorbed on bilayer BP, from physisorption to chemisorption. b) Snapshots of ABMD simulations of H_2O on oxygen adsorbed bilayer BP. The P–P bond of the top layer breaks and leads to the breakdown of BP after 1.5 ps. O Red, H white, P purple.

words, on account of the strong Coulomb interaction between O_2^- and p-typed BP, the reaction barrier should be even lower in reality. Moreover, the final state via the reaction path of dissociation of O_2^- is about 1 eV lower than that of O_2, suggesting that the formation of O_2^- facilitates the oxidation of BP.

The last step of degradation of BP is the dissolution of O adsorbed phosphorene in water. To model this process, we placed a water molecule onto the oxidized BP (Figure 2b). The H atom of water is connected to one of the O atoms via a hydrogen-bond (H-bond). Room temperature ABMD simulations show that, after about 1.3 ps, one of the dangling O atoms and its bonded P atom are lifted off the surface by the dragging of H_2O. The P–P bond connected to the lower P is broken. This reduces the structural stability and leads to a reconstruction of the neighboring P atoms after a short time. Although the water molecule does not actually remove the P atoms off the surface during our simulation time (5 ps), the distortion caused by the water molecule does not recover either. We believe it will eventually disintegrate in a real time scale or with the help of other water and oxygen molecules. The second layer is intact during the simulation also indicates that the degradation process is not simultaneous but layer-by-layer.

Now we can have a clear picture on the few-layer BP degradation. First of all, the superoxide anions are generated through a charge transfer reaction on the surface of BP under ambient light (Figure 1a, Step I). The thickness-dependent band gaps and conduction band edges lead to different surface oxygen concentrations on the thinner and thicker BP. Then the superoxide anions overcome a small barrier and form dangling O atoms at the surface via a triplet–singlet conversion (Step II). These dangling O atoms make the surface highly hydrophilic. Finally, through the H-bond interaction, the H_2O molecules draw the bonded O out of the surface and subsequently remove the connected P atoms (Step III), which leads to the dissolution of the top-layer and further oxidation of the next layer. This degradation mechanism unveiled herein corroborates the conclusions drawn experimentally[5] and successfully addresses the conflicting in different studies.[3,4,6]

As discussed above, the oxidation alone does not break down the structure of phosphorene. However, when the water is involved, the stability of the surface is challenged by the H-bond interaction between dangling O and H_2O, and the initial collapse begins with the P–P bond breaking (Figure 3a). The average P–P bond length in monolayer BP is 2.248 Å, which is not very strong. On the other hand, P atoms can form a stronger covalent bond with O atoms. If the P–P bonds are replaced by the P–O–P bonds (Figure 3b), the hydrophilic surface will be largely stabilized and have a great opportunity to survive the collapse. Thus, through a fully surface oxidation, the phosphorene oxide is expected to turn into a protective layer.

ABMD simulation was carried out to evaluate the thermal stability of fully oxidized phosphorene in the presence of H_2O. The fully oxidized structure is taken from the stable layered structure of o'-P_2O_5.[16] The optimized average P–O bond is 1.596 Å, which is much shorter than the P–P bond in

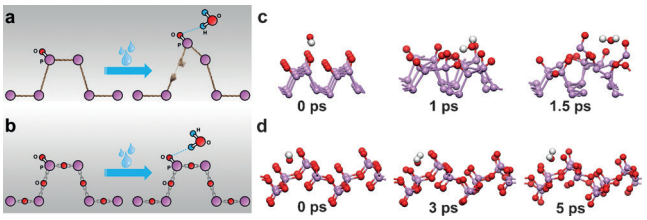

Figure 3. Left: The stability of BP with a) P–P and b) P–O–P bonding in the presence of water. The bridging O between P atoms helps to stabilize the surface of BP framework. Right: Snapshots of ABMD simulations of H_2O adsorbed on c) partial and d) fully oxidized phosphorene monolayer. The partial oxidized layer without P–O–P bond breaks down after 1.5 ps, while the fully oxidized layer maintains its integrity during the simulation time (5 ps).

phosphorene. Figure 3d shows that the H-bonds between H and O keep the adsorbed H_2O near the surface, but it does not break any bond, and the oxide monolayer maintains its integrity during the simulation time (5 ps). This is consistent with the experimental observation of stable oxide at the surface of bulk BP.[8] The high stability of the fully oxidized phosphorene is derived from the formation of bridge P–O–P bonds. On the contrary, for partial oxidized phosphorene without the formation of P–O–P bonds, the adsorbed H_2O distorts the O-covered surface and leads to the break of P–P bonds in a short time (Figure 3c). In fact, if the bridge P–O–P bonds are widely formed, the surface of partial oxidized BP with the same oxidation degree is no longer easy to break (Supporting Information, Figure S5). Therefore, the structural collapse of few-layer BP in the ambient environment should happen at the moment the top-layer is just slightly oxidized, that is, no or very few P–O–P bonds are formed. The oxidization process in environment is not fast enough to form a fully-oxidized layer before it is torn up by water. We expect an intentional water-free oxidization (such as ozone treatment or other controllable oxidization process) can help to form a fully oxidized native protective layer on the top of phosphorene.

In the end, we investigate the electronic properties of phosphorene oxide. The HSE band structure of P_2O_5 monolayer shows an extremely large direct band gap of 7.2 eV (Figure 4a), which gives it no chance to produce excitons under ambient light. And because of its transparency, the photoelectric properties of BP underneath will not be affected. The PBE band structure of bilayer BP capped with P_2O_5 monolayer exhibits a direct band gap of 0.36 eV at the Γ point, which is close to the value of bare bilayer BP (Table 1). The hybridization of the oxide layer and the bilayer BP beneath only happens on the conduction bands (Figure 4c) and the effective mass in the Γ-X direction slightly increases. Moreover, the valence bands are almost unchanged, the effective mass of hole in the VBM is thereby kept in both directions. Therefore, the high hole mobility of phosphorene is maintained intact when a fully oxidized layer is capped (Table 1). Additionally, the hole mobility in the armchair direction is even increased a little. This is mainly the consequence of the enlarged thickness brought by the extra oxide layer (Supporting Information, Table S3).

Table 1: Bandgap and hole mobility of bilayer BP without/with capping oxide layer.[a]

Structures	Bandgap [eV]	C_x	C_y [J m^{-2}]	E_{1x}	E_{1y} [eV]	m_x^*/m_0 G-X	m_y^*/m_0 G-Y	μ_x	μ_y [10^3 cm^2 V^{-1} s^{-1}]
2ML	0.43	59.85	199.06	3.25	1.57	0.10	2.08	2.54	1.78
P_2O_5@2ML	0.36	77.11	313.04	3.32	2.36	0.10	2.09	3.25	1.24

[a] C_x(C_y), E_{1x}(E_{1y}) and m_x^*(m_y^*) are 2D elastic modulus, deformation potential, and hole effective mass for the x(y) directions, respectively. Hole mobilities μ_x and μ_y are calculated at a temperature of 300 K.

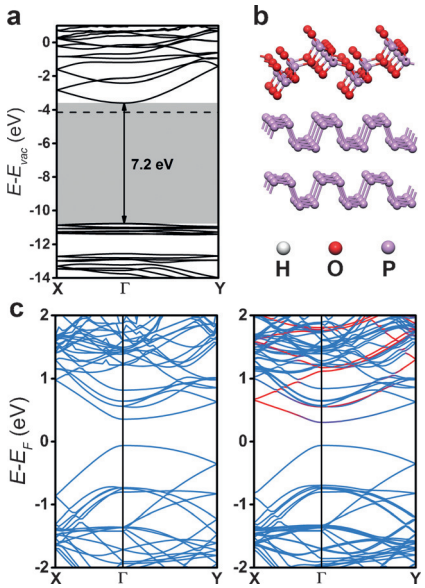

Figure 4. a) HSE band structures of P_2O_5 monolayer. b) Atomic structure of bilayer BP capped with its oxide monolayer. c) PBE band structures of bilayer BP without/with its oxide. The contribution of the capped oxide layer is marked red. The fully oxidized capping layer has little effect on the band structure of bilayer BP underneath.

In summary, a comprehensive picture on the phosphorene ambient degradation has been built up, and the roles of light illumination, oxygen, and water in degradation have been explicitly expounded. The formation of the superoxide anions at the surface is vital and accelerates the oxidation of thinner BP. The well-matched band gap and band-edge positions for the redox potential are responsible for thickness-dependent degradation behavior. We further demonstrate that a fully surface oxidization treatment can effectively prevent few-layer BP from deterioration and leave the underneath BP intact with high hole mobility simultaneously. This study provides a profound understanding on the degradation mechanism and opens a possible route to stabilize BP against air and water.

Acknowledgements

This work is supported by the NSFC (21525311, 21373045, 11404056), the NSF of Jiangsu (BK20130016), the SRFDP (20130092110029, 20130092120042), and the Fundamental Research Funds for the Central Universities of China. The authors thank the computational resources at the SEU and National Supercomputing Center in Tianjin.

Keywords: ab initio calculations · black phosphorus · degradation · oxidization · protection

How to cite: *Angew. Chem. Int. Ed.* **2016**, *55*, 11437–11441
Angew. Chem. **2016**, *128*, 11609–11613

[1] a) A. Castellanos-Gomez, *J. Phys. Chem. Lett.* **2015**, *6*, 4873; b) L. Z. Kou, C. F. Chen, S. C. Smith, *J. Phys. Chem. Lett.* **2015**, *6*, 2794; c) H. Liu, Y. C. Du, Y. X. Deng, P. D. Ye, *Chem. Soc. Rev.* **2015**, *44*, 2732; d) M. Wu, H. Fu, L. Zhou, K. Yao, X. C. Zeng, *Nano Lett.* **2015**, *15*, 3557.

[2] a) L. K. Li, Y. J. Yu, G. J. Ye, Q. Q. Ge, X. D. Ou, H. Wu, D. L. Feng, X. H. Chen, Y. B. Zhang, *Nat. Nanotechnol.* **2014**, *9*, 372; b) J. S. Miao, S. M. Zhang, L. Cai, M. Scherr, C. Wang, *ACS Nano* **2015**, *9*, 9236; c) J. Na, Y. T. Lee, J. A. Lim, D. K. Hwang, G. T. Kim, W. K. Choi, Y. W. Song, *ACS Nano* **2014**, *8*, 11753; d) J. S. Qiao, X. H. Kong, Z. X. Hu, F. Yang, W. Ji, *Nat. Commun.* **2014**, *5*, 4475.

[3] a) A. Castellanos-Gomez, L. Vicarelli, E. Prada, J. O. Island, K. L. Narasimha-Acharya, S. I. Blanter, D. J. Groenendijk, M. Buscema, G. A. Steele, J. V. Alvarez, H. W. Zandbergen, J. J. Palacios, H. S. J. van der Zant, *2D Mater.* **2014**, *1*, 025001; b) J. O. Island, G. A. Steele, H. S. J. van der Zant, A. Castellanos-Gomez, *2D Mater.* **2015**, *2*, 011002; c) S. P. Koenig, R. A. Doganov, H. Schmidt, A. H. C. Neto, B. Ozyilmaz, *Appl. Phys. Lett.* **2014**, *104*, 103106.

[4] A. Ziletti, A. Carvalho, D. K. Campbell, D. F. Coker, A. H. C. Neto, *Phys. Rev. Lett.* **2015**, *114*, 046801.

[5] A. Favron, E. Gaufres, F. Fossard, A. L. Phaneuf-L'Heureux, N. Y. W. Tang, P. L. Levesque, A. Loiseau, R. Leonelli, S. Francoeur, R. Martel, *Nat. Mater.* **2015**, *14*, 826.

[6] G. Wang, W. J. Slough, R. Pandey, S. P. Karna, *2D Mater.* **2016**, *3*, 025011.

[7] a) J. S. Kim, Y. N. Liu, W. N. Zhu, S. Kim, D. Wu, L. Tao, A. Dodabalapur, K. Lai, D. Akinwande, *Sci. Rep.* **2015**, *5*, 8989; b) J. D. Wood, S. A. Wells, D. Jariwala, K. S. Chen, E. Cho, V. K. Sangwan, X. L. Liu, L. J. Lauhon, T. J. Marks, M. C. Hersam, *Nano Lett.* **2014**, *14*, 6964; c) A. Avsar, I. J. Vera-Marun, J. Y. Tan, K. Watanabe, T. Taniguchi, A. H. C. Neto, B. Ozyilmaz, *ACS Nano* **2015**, *9*, 4138; d) X. L. Chen, Y. Y. Wu, Z. F. Wu, Y. Han, S. G. Xu, L. Wang, W. G. Ye, T. Y. Han, Y. H. He, Y. Cai, N. Wang, *Nat. Commun.* **2015**, *6*, 7315; e) R. A. Doganov, E. C. T. O'Farrell, S. P. Koenig, Y. T. Yeo, A. Ziletti, A. Carvalho, D. K. Campbell, D. F. Coker, K. Watanabe, T. Taniguchi, A. H. C. Neto, B. Ozyilmaz, *Nat. Commun.* **2015**, *6*, 6647; f) Y. Zhao, H. Wang, H. Huang, Q. Xiao, Y. Xu, Z. Guo, H. Xie, J. Shao, Z. Sun, W. Han, X. Yu, P. Li, P. K. Chu, *Angew. Chem. Int. Ed.* **2016**, *55*, 5003–5007; *Angew. Chem.* **2016**, *128*, 5087–5091; g) C. R. Ryder, J. D. Wood, S. A. Wells, Y. Yang, D. Jariwala, T. J. Marks, G. C. Schatz, M. C. Hersam, *Nat. Chem.* **2016**, *8*, 597.

[8] M. T. Edmonds, A. Tadich, A. Carvalho, A. Ziletti, K. M. O'Donnell, S. P. Koenig, D. F. Coker, B. Ozyilmaz, A. H. C. Neto, M. S. Fuhrer, *ACS Appl. Mater. Interfaces* **2015**, *7*, 14557.

[9] J. J. Pei, X. Gai, J. Yang, X. B. Wang, Z. F. Yu, D. Y. Choi, B. Luther-Davies, Y. R. Lu, *Nat. Commun.* **2016**, *7*, 10450.

[10] a) G. Kresse, J. Furthmuller, *Phys. Rev. B* **1996**, *54*, 11169; b) G. Kresse, J. Furthmuller, *Comp. Mater. Sci.* **1996**, *6*, 15.
[11] J. P. Perdew, K. Burke, M. Ernzerhof, *Phys. Rev. Lett.* **1996**, *77*, 3865.
[12] a) J. Heyd, G. E. Scuseria, M. Ernzerhof, *J. Chem. Phys.* **2003**, *118*, 8207; b) J. Heyd, G. E. Scuseria, M. Ernzerhof, *J. Chem. Phys.* **2006**, *124*, 219906.
[13] a) J. Klimes, D. R. Bowler, A. Michaelides, *Phys. Rev. B* **2011**, *83*, 195131; b) J. Klimes, D. R. Bowler, A. Michaelides, *J. Phys. Condens. Matter* **2010**, *22*, 022201.
[14] G. Henkelman, B. P. Uberuaga, H. Jonsson, *J. Chem. Phys.* **2000**, *113*, 9901.
[15] P. W. Bridgman, *J. Am. Chem. Soc.* **1914**, *36*, 1344.
[16] D. S. Stachel, I. Svoboda, H. Fuess, *Acta Crystallogr. Sect. C* **1995**, *51*, 1049.

Received: May 27, 2016
Published online: August 16, 2016

